Chen, Y.; Lu, X.; Blawert, C.; Zheludkevich, M.L.; Zhang, T.; Wang, F.:
Formation of self-lubricating PEO coating via in-situ incorporation of PTFE particles
In: Surface and Coatings Technology 337 (2018) 379 - 388
First published online by Elsevier: January 09, 2018

DOI: 10.1016/j.surfcoat.2018.01.022
https://doi.org/10.1016/j.surfcoat.2018.01.022

Formation of self-lubricating PTFE-containing PEO coating via in-situ incorporation

Yan Chen[1,3,4], Xiaopeng Lu[2,3*], Carsten Blawert[3], Mikhail L. Zheludkevich[3], Tao Zhang[1,2*], FuhuiWang[1,2]

[1] *Laboratory for Corrosion and Protection, Institute of Metal Research, Chinese Academy of Sciences, Wencui Road 62, Shenyang, 110016, China*

[2]*Key Laboratory for Anisotropy and Texture of Materials, Education Ministry of China, School of Material Science and Engineering, Northeastern University, 3-11 Wenhua Road, Shenyang 110819, China*

[3]*Institute of Materials Research, Helmholtz Zentrum Geesthacht, Max-Plank-Str. 1, Geesthacht, 21502, Germany*

[4] *University of Chinese Academy of Sciences, Yuquan Road 19, Beijing, 110049, China*

Abstract

A self-lubricating PTFE-containing PEO coating was successfully fabricated on AZ91 magnesium alloy via in-situ incorporation methods. Study of SEM, EDS mapping, XRD and wear behaviour indicated that the fabricated PEO coatings show a high degree of sealing and superior tribological properties compared with the particle-free coating. Further study of the coating surface after different treatment times demonstrates that ridge-like PTFE-enriched protrusions can act as load-bearing zones during sliding wear test and provide super self-lubricating capability for PEO coating. The appearance of the protrusions are likely due to gas microbubbles sticking to the surface due to high viscosity of the electrolyte containing PTFE. As a consequence, the intensity of electric field at the edge of the bubbles increases, followed by more

intensive arcing and induced rapid sintering of PTFE particles at the electrolyte/gas/coating interface.

Keywords: Magnesium; Plasma electrolytic oxidation; PTFE; Tribological property.

1. Introduction

Plasma electrolytic oxidation (PEO) is one promising surface treatment process, which can produce electrically insulating ceramic-like coating on light metals and their alloys (Al, Mg and Ti) [1,2]. PEO coatings are usually produced from eco-friendly alkaline electrolytes under high voltage, accompanied by numerous short-lived discharges [3] [4]. The properties of PEO coatings mainly depend on electrolyte, treatment time, temperature, and electrical parameters [5-7], where the composition of the electrolyte have predominant effect due to direct incorporation of species from the bath into the oxide coating [8,9].

However, due to the high porosity and roughness as well as limited range of phase compositions, PEO coatings are unable to provide long-term wear protection [10-12]. Recently, introducing hard ceramic particles (SiC, TiO_2, Al_2O_3, etc.) or self-lubricating organic particles into the coatings have been considered as a possibility to increase the wear resistance of the coating [13-15]. Among them, polytetrafluoroethylene (PTFE) is usually adopted to effectively enhance the tribological property of the coating, either by ex-situ or in-situ infiltration methods. The ex-situ technology utilizes post-treatment of previously formed PEO coatings [16-18]. Gnedenkov et al. [17] carried out the

potentiostatically electrophoretic deposition method to grow a homogeneous PTFE layer on a base PEO coating. The composite coating effectively reduces the corrosion current density and the wear rate compared to that of the blank PEO coating. In order to improve the efficiency of particle incorporation, Wang et al. [18] has deposited a Al_2O_3/PTFE composite coating in low vacuum atmosphere which confers superior tribological properties.

so far, there are only a limited number of reports about an in-situ incorporation of PTFE particles by direct addition to the PEO electrolytes [19-20]. Chen et al. [19] introduced Al_2O_3 and PTFE particles to Al anodized, and found that the synthesized coating demonstrate both high hardness and desirable anti-wear property. Similar study has been performed by Guo et al. [20] using a PTFE-containing solution to produce a novel PEO coating with good hydrophobic property as well as wear performance. However, the uptake mechanism of the PTFE particles together with the coating growth process has not been fully understood.

It should be noted that PTFE particles have some unique physical characteristics which might render them different from the aforementioned ceramic particles in the formation of PEO coatings via in-situ incorporation. On the one hand, strong hydrophobicity of PTFE remains a barrier to uniform distribution of particles in the coating. This can be improved by surfactants which will nevertheless inevitably change the composition of the electrolyte. On the other hand, the low melting point of PTFE

(327 °C) is also an issue to be used during PEO treatment as the melting point of the particles plays an important role in the incorporation mode [21]. In most of the previous studies, the particles used have relatively high melting point, for example, SiC (2730 °C), Si_3N_4 (1900 °C) and clay (between 1000 and 1200 °C). Hence, PEO process in PTFE-containing electrolyte is more complicated from practical and theoretical aspects.

In the present work, a novel PTFE-containing composite coating has been successfully fabricated via an in-situ method. Investigation of the effects of nano-sized PTFE particles addition on the PEO process, coating morphology, phase composition and tribological properties of PEO coatings is presented. The uptake and incorporation mechanism of the PTFE particles is also proposed herein.

2. Experimental

Specimens of the Mg alloy AZ91 with dimensions of 15 mm × 15 mm × 4 mm were cut from gravity cast ingot material. The chemical composition of the AZ91 alloy, as measured with an Arc Spark OES (Spark analyser M9, Spectro Ametek, Germany), is 8.34 wt.% Al, 0.56 wt.% Zn, 0.236 wt.% Mn, 0.066 wt.% Si, 0.002 wt. % Fe, 0.005 wt.% Cu and Mg balance. The specimens were ground using SiC abrasive papers up to 1200 grit, rinsed with ethanol and then air-dried prior to PEO treatment.

The PEO process was performed by using a standard lab-produced DC power supply (PS 8000 2U, ELEKTRO AUTOMATIK, Germany) with a self-made pulsing unit.

The pulse ratio of t_{on}:t_{off} was adjusted to 0.4 ms:3.6 ms. The specimen and a stainless steel tube were used as the anode and cathode, respectively. The temperature of the electrolyte was maintained at 20 ± 2℃ by a water cooling system. 20g/l of nano-sized PTFE particles (33.3 g/l 60 wt.% PTFE suspension solution from Sigma-Aldrich Company) were added to a base phosphate-based electrolyte (20 g/l Na_3PO_4 and 10 g/l KOH). A stirrer and bubbling generator were used to facilitate the uniform distribution of the particles in the electrolyte. PEO coatings were produced under a constant voltage (300V) regime for 5min and the maximum average current density was limited to 150 mA/cm^2. A scanning electron microscope (TESCAN Vega3 SB) combined with an energy dispersive spectrometer (EDS) system from eumeX (IXRFsystems) was used to examine the microstructure and composition of the PEO coatings. An acceleration voltage of 15 kV was applied for SEM and EDS investigations. Commercial software Alicona Mex was used for reconstructing surface topography based on calculation of two high resolution SEM images obtained under a tilting angle of 10°. ImageJ software was used to measure the pore characteristics. X-ray diffraction (XRD) under glancing angle mode (3°) was performed using a diffractometer (D8 Advance, Bruker AXS) equipped with Cu Ka radiation to determine the coating phase composition. The measurements were performed at 40 kV voltage and 40 mA current, with a step size of 0.02° and 1 s for each step.

Additionally, the dry sliding wear behavior of the PEO coatings was assessed with a Tribotec ball-on-disc oscillating tribometer with an AISI 52100 steel ball of 6mm

diameter as static friction partner. The wear tests were performed at ambient conditions (25 ± 2℃ and 30 % r.H.) under 5 N load with an oscillating amplitude of 10 mm at a sliding velocity of 5 mm s^{-1}, for a sliding distance of 12m.

3. Results

3.1 Microstructure

Fig. 1 shows SEM image of PTFE particles from the dried commercial suspension solution. It can be seen that size of the particles is in the range of 180~240 nm. Nonionic surfactants (Poly(oxy-1,2-ethanediyl) and α-[3,5-dimethyl-1-(2-methylpropyl)hexyl]-ω-hydroxyl) in the solution are used to disperse uniformly the nanoparticles and improve the stability of the suspension system. The mechanism is that the hydrophobic groups of the surfactants adsorb on the surface, and a hydrated film is formed to envelop the PTFE particle which changes the surface polarity and significantly reduces the surface tension of the nanoparticles.

The change of current as a function of treatment time under constant voltage regime with and without PTFE particle addition is shown in Fig. 2. The particle addition significantly influences the evolution of the current. For the coating without particles, the current continuously decreases during the whole PEO process, indicating the formation of a passive and insulating film on the surface. After adding particles in the electrolyte, the current decreases faster in the initial stage of anodization and remains stable at a relatively low value due to the formation of a barrier type oxide film on the

surface of specimen. However, after 3 min, the current starts ramping again accompanied by severe sparking and acoustic phenomenon. This is probably owing to the formation of severe stationary discharges around bubbles attached on the surface.

3.1.1 Surface morphology

Fig. 3 presents the surface morphology of coatings without and with PTFE particle addition after 5-min PEO treatment. The former coating (Fig. 3a) shows more number of large sized pores compared to the particle-containing coating (Fig. 3b). In Fig. 3c, numerous cracks can be observed for the coating without particles probably due to the thermal stress induced by rapid cooling of the melted coating materials. Interestingly, addition of particles demonstrates efficient sealing effect on the coating surface, reducing pore size and open porosity in general. Additionally, ridge-like semicircle protrusions can be observed with 300~400 μm in diameters (Fig. 3d). 3D images acquired by Alicon Mex software are shown in Fig. 4 to model the topography of the surface of the coating in the presence of particles. It can be clearly seen that two ring-like ridges protruding from the horizontal plane. The surface profile along the red line demonstrates that the height of the protrusions is around 20~30 μm.

To correlate the coating evolution process with current response, the surface morphology of coatings with PTFE particles at different times (1 min, 2min, 3min and 5min) are shown in Fig. 5. After 1 min treatment (Fig. 5a), the whole surface is dominated by a large number of fine pores which are characteristic of PEO coatings.

With prolonged treatment time, the open pores are less but bigger in size, as indicated in Fig. 5(b) and (c). At the end of 5min (Fig. 5d), the coating surface reveals a high degree of sealing, exhibiting a smallest open porosity (0.932%) compared to the other three coatings (1 min (4.125%), 2min (2.537%), 3min (1.262%)). Together with the change of porosity, the overall morphology for PEO coatings is also changing from the typical wavy protrusions based morphology to a scaly appearance.

3.1.2 Cross section

Fig. 6 shows backscattered electron (BSE) micrographs for the cross section of the PEO coatings treated for different times. Before the current ramp again ($\leqslant$3min), the coating grows uniformly and becomes thicker from around 5 to 12 μm, as shown in Fig. 6 (a), (b) and (c). However, , the coating starts to be very inhomogeneous after 5 min, which can be correlated to the protrusions corresponding well to the ridge-like regions observed on the surface. The coating thickness ranges from 20 μm to around 45 μm. In addition, coating underlying the protrusions seems to have a stronger tendency to grow inwards compared to the adjacent area. To trace the distribution of PTFE particles through the coatings, EDS mapping and line scan of F element (indicated by red dotted rectangles and red solid lines, respectively) are performed. Both results demonstrate that the particles are not randomly distributed in the coatings. In the first 3 min, the resultant coatings have F-enriched areas well-matching the locations of open pores and a distinctly F-enriched layer in the coating/substrate

interface. The observed phenomenon is somehow different from previous studies where the elements from the incorporated particles are normally more uniformly distributed in the coatings [22, 23]. This might be due to the various properties of the particles, e.g. melting point, electrophoretic mobility and size. Nevertheless, for the coating treated for 5min, high amount of F species can be detected on the outer layer of protrusions, which may result from the sintering of PTFE particles under severe sparking.

3.2 Phase and chemical composition

The X-ray diffraction patterns of the coatings treated for different times are depicted in Fig. 7. The appearance of α Mg peaks in all conditions is from the substrate due to the penetration of the X-ray through the oxide layer. It can be seen that without particles, the coating is composed of a nano-crystalline and/or amorphous phase in the 2θ range of 20~35°, possibly originated from phosphate phase, and a relatively high amount of MgO. Distinct PTFE peaks are visible after adding particles into the electrolytes, indicating that a part of the nano-sized particles are inertly incorporated into PEO coating. In addition, increasing treatment time leads to a higher ratio of PTFE peaks compared to MgO peaks. In order to study the evolution process of particle uptake, EDS analysis was performed on the surface of coated specimens and the F, P and O content (wt.%) is presented in Fig. 8. It is found that the longer treatment time enables PEO coating to incorporate more PTFE particles, especially after 3 min. After the

current ramp occurred, the amount of F for the 5 min-treated specimen (38.3%) is almost twice as high as that of 3 min (21.5%).

3.3 Tribological performance

The evolution of the friction coefficient determined for the aforementioned coatings and AZ91 substrate against AISI 52100 steel ball is shown in Fig. 9. In the first 1 m of sliding, the friction coefficient is observed to rapidly rise to 0.64 and ends at 0.77 for PEO coating without particles, indicating fast abrasion of the coating under unlubricated conditions. The surface morphology of the corresponding counterparts (steel ball) is presented in Fig. 10(a). Flattened worn surfaces with obvious scratches can be observed, indicating the steel ball has suffered abrasive wear damage against the PEO coatings. The coatings produced in PTFE-containing electrolytes after different treatment times demonstrate enhanced wear resistance to a certain extent. The friction coefficient value of 1min-treated coatings increases to around 0.61 in the first 6 m of sliding, followed by a large oscillation in the range of 0.30-0.68 for the remaining distance. The severe fluctuation is mostly likely related to the partial exposure of the Mg substrate after grinding away most of the thin PEO layer. The 2min-treated specimen shows similar tendency as the 1min-treated coating, but a much lower friction coefficient value due to the self-lubricant effect of higher amount of incorporated PTFE particles. As for coating anodized for 3 min, friction coefficient increases slowly and reaches a steady-state value of 0.44 until the end of sliding

distance. This is a clear indication that there was no coating failure. PEO coating after 5min treatment shows the best wear resistance characterized by a low and stable friction coefficient (approximately 0.08) during the overall sliding test. Meanwhile, Fig. 10(b) reveals that the surface of counterpart sliding against the PEO-coated specimen is smooth and flat with few discontinuous residuals. Further point EDS analysis located by the red cross shows high P and O content for the residual material compared to surrounding area, which can result from the fragmented PEO coatings. It could be inferred that the prominent improvement in tribological performance can be attributed to the presence of the PTFE-enriched ridge-like protrusions.

The morphology and EDS mapping for the wear tracks of the PEO coatings with PTFE addition slid against the steel ball are shown in Fig. 11. The wear track of the 1min-treated specimen (Fig. 11a) is broad and deep, characterized by many grooves and scratch marks parallel to the sliding direction. Almost no P or F elements can be detected in the wear track of the, indicating that coating has been completely removed during the wear test. This is consistent with the recorded friction coefficient. As displayed in Fig. 11 (b) and (c), after longer treatment time (2min and 3min), larger amount of coating materials, especially F element, in the wear tracks demonstrate less appreciable coating removal and improved wear resistance. For the 5min-treatd coating (Fig. 11d), slightly worn protrusions remain on the surface after wear test and surrounding coatings seem to be totally intact. In order to understand the effect of ridge-like protrusions during sliding, 3D SEM image of PEO coating acquired after dry

sliding are shown in Fig. 12. It is obvious that only the top of the ridge-like protrusions is worn away. The surface profile located by the red line demonstrates that the remained height of the protrusion is around 10~15 μm compared to the adjacent horizontal plane. EDS mapping of the cross-section of the coating through the wear track (Fig. 13) indicates that plenty of F-containing materials still exist on the surface of protrusions, encompassing a F-free coating in the center. It is evident that the PTFE-enriched ridge-like areas can act as load-bearing regions during the wear test, which endow coatings with excellent self-lubricant abilities.

4. Discussion

The addition of PTFE particles into the electrolytes notably changes the microstructure, wear resistance and formation mechanism of composite PEO coatings. Under constant-voltage mode, PEO process in PTFE-containing electrolyte exhibits abnormal phenomena characterized by severe sparking and current ramping after a previous decrease in current. This leads to formation of coating with PTFE-enriched ridge-like protrusions which can act as load-bearing points and confer superior tribological properties.

In previous studies regarding PEO process where micro- or nano-particles are added in the electrolyte, the resultant coatings demonstrate a homogeneous distribution of particles in the cross-sectional microstructure [22, 23]. However, in the presented work, F element, which is related with PTFE particles, displays enrichment in certain regions

in the coating after different treatment time. Before the current ramp, the EDS mapping (Fig. 6) reveals a F-enriched layer in the interface of the coating and substrate. This might be due to the particular hydrophobicity of the PTFE particles. Since the surfactants used in the suspension solution are non-ionic type with no charge, they merely assist in dispersing the particles by forming a hydrated outer layer without changing the electric potential of the particles [24]. Therefore, under the electric field built up between the anode and cathode, the particles hardly move towards any side, resulting in uneven distribution in the coating. In addition, during PEO process, the originally formed thin film will be punctured after breakdown phenomena, accompanied by numerous microdischarges. Under the high pressure and temperature induced by the discharges, the PTFE particles characterized by a low melting point (327 °C) will decompose, as indicated in the following reaction [25],

$$-(CF_2\text{-}CF_2)_n- \rightarrow CF_4 + HF + CF_3CF{=}CF_2 \quad (1)$$

The small amount of hydrogen fluoride generated will be rapidly dissolved and neutralized by the alkaline electrolyte. Thus, anodizing in F^--containing solution can lead to formation of a compact MgF_2 inner layer in the interface between coating and substrate due to high thermodynamical stability of MgF_2 [26, 27]. This can explain why the coating treated after 1, 2 and 3 min in the PTFE-containing solution has a F-enriched inner layer. It should be noted that a certain amount of particles which have not decomposed will be incorporated into the coating via discharge channels and open

pores. This corresponds with the high signal of F element in the aforementioned regions and will result in the enhanced wear resistance of the coating.

Nevertheless, for the coating treated for 5min, a high amount of F-containing species can be detected in the top layer, especially of the protrusions, apparently formed by different mechanism. Since the diameter of the ridge-like semicircle protrusions is approximately 300~400 μm, it is likely that the formation of this macro-sized structure is due to the bubbles generated by the PEO process. Due to changed surface energy influenced by the surfactants and/or higher viscosity owing to the particles, those bubbles can stick on the surface for longer time. Fig. 14 illustrates the schematic diagram of formation mechanism of the ridge-like protrusions during PEO process. In the initial stage of the PEO process (before current ramp), the coating grows homogenously (Fig. 14a). The PTFE particles are partly incorporated into the open pores via large discharge channels or enter the coating/substrate interface as F ion (decomposition product) forming a MgF_2-enriched interface. As PEO process is accompanied by vigorous oxygen evolution resulting from electrochemical reaction and thermo-decomposition of water, the newly formed oxygen will provide new bubbles. Thus, with increasing treatment time, more oxygen microbubbles will accumulate on the sample surface and start to merge into large bubbles (Fig. 14b). The existence of the bubbles will lead to increased intensity of electric field at the edge of the bubbles where electrical potential lines converge due to the increased curvature. Clearly, field-assisted discharges will occur at the periphery of the bubbles and induce

high temperature and pressure which benefit rapid growth of coating and in-situ sintering of PTFE particles (Fig. 14c). This explanation accounts for the ridge-like protruding structure of the coating and accounts for the superior wear resistance of the resultant PEO coating.

During the tribological tests, the distribution and amount of the PTFE particles in the coating greatly influence its wear behavior. Regarding the coatings treated for 1, 2 and 3 min, respectively, the friction coefficient decreases gradually since the amount of PTFE particles is increasing in and on the surface (Fig. 8). During the wear tests, the solid lubricant particles stored in the micro-pores can move to the top surface and the extended chain linear molecules will form low shear strength films in dry sliding test, resulting in lower friction coefficient compared to coating without particles [28, 29]. In comparison, after formation of the ridge-like protrusions with enriched PTFE content (coating anodized for 5 min), those regions will act as load-bearing points and contact zones, preventing the surrounding coating from direct rubbing with the steel ball during the wear test.

In order to prove the ring-like protruding are related with the microbubbles adhered on the sample surface, an additional bubbling generator was set below the sample to remove them by producing vigorous bubbles. Under this circumstance, the current gradually decreased during 5-min PEO treatment. Fig. 15(a) shows the surface morphology of the coating with bubbling, where no typical semicircle ridges can be

observed. As expected, the continuously increasing friction coefficient of the coating (as indicated in Fig. 15b) demonstrates the deteriorated wear resistance compared yo the coating with those protrusions. This phenomenon further proves the theory proposed that the occurrence of the ring-like ridges is due to long staying microbubbles and contributes significantly to enhancing the tribological properties of the resultant coating.

5. Conclusion

In the present study, a self-lubricating PTFE-containing PEO coating was successfully produced on AZ91 magnesium alloy via in-situ incorporation methods. The deposited coating shows a high degree of sealing and superior tribological property compared with the pure PEO coating. Inspection of 3D SEM and EDS mapping analysis indicated that the semi-circle PTFE-enriched protrusions can act as load-bearing zones, preventing the surrounding coating from direct contact with the steel ball during the wear test. In addition, the ridge-like protrusions are likely due to the existence of microbubbles on the sample surface which leads to increased intensity of electric field at the edge and induces rapid sintering of coating and PTFE particles on top.

Acknowledgements

The technical support of Mr. Volker Heitmann and Mr. Ulrich Burmester during this work is gratefully acknowledged. Yan Chen thanks Chinese Academy of Sciences and German Academic Exchange Service for the jointed CAS-DAAD scholarship.

References

[1] R. Arrabal, E. Matykina, F. Viejo, P. Skeldon, G.E. Thompson, Corrosion resistance of WE43 and AZ91D magnesium alloys with phosphate PEO coatings, Corros. Sci. 50 (2008) 1744–1752.

[2] Y. Zhang, C. Yan, F. Wang, H. Lou, C.-N. Cao, Study on the environmentally friendly anodizing of AZ91D magnesium alloy, Surf. Coat. Technol. 161 (2002) 36–43.

[3] L. Liu, Y. Li, F. Wang, Influence of grain size on the corrosion behavior of a Ni-based superalloy nanocrystalline coating in NaCl acidic solution, Electrochimi. Acta. 53 (2008) 2453–2462.

[4] C. Blawert, W. Dietzel, E. Ghali, G. Song, Anodizing Treatments for Magnesium Alloys and Their Effect on Corrosion Resistance in Various Environments, Adv. Eng. Mater. 8 (2006) 511–533.

[5] R. Arrabal, E. Matykina, T. Hashimoto, P. Skeldon, G.E. Thompson, Characterization of AC PEO coatings on magnesium alloys, Surf. Coat. Technol. 203 (2009) 2207–2220.

[6] S.V. Gnedenkov, O.A. Khrisanfova, A.G. Zavidnaya, S.L. Sinebryukhov, V.S. Egorkin, M.V. Nistratova, et al., PEO coatings obtained on an Mg–Mn type alloy under unipolar and bipolar modes in silicate-containing electrolytes, Surf. Coat. Technol. 204 (2010) 2316–2322.

[7] A.V. Timoshenko, Y.V. Magurova, Investigation of plasma electrolytic oxidation processes of magnesium alloy MA2-1 under pulse polarisation modes, Surf. Coat. Technol. 199 (2005) 135–140.

[8] M. Mohedano, E. Matykina, R. Arrabal, A. Pardo, M.C. Merino, Metal release from ceramic coatings for dental implants, Dent. Mater. 30 (2014) e28–e40.

[9] X. Lu, S.P. Sah, N. Scharnagl, M. Störmer, M. Starykevich, M. Mohedano, et al., Degradation behavior of PEO coating on AM50 magnesium alloy produced from electrolytes with clay particle addition, Surf. Coat. Technol. 269 (2015) 155–169.

[10] H. NasiriVatan, R. Ebrahimi-Kahrizsangi, M.K. Asgarani, Tribological performance of PEO-WC nanocomposite coating on Mg Alloys deposited by Plasma Electrolytic Oxidation, Tribiol. Int. 98 (2016) 253–260.

[11] R.O. Hussein, D.O. Northwood, J.F. Su, X. Nie, A study of the interactive effects of hybrid current modes on the tribological properties of a PEO (plasma electrolytic oxidation) coated AM60B Mg-alloy, Surf. Coat. Technol. 215 (2013) 421–430.

[12] J. Guo, L. Wang, J. Liang, Q. Xue, F. Yan, Tribological behavior of plasma electrolytic oxidation coating on magnesium alloy with oil lubrication at elevated temperatures, J. Alloys Compd. 481 (2009) 903–909.

[13] Y. Yang, H. Wu, Effects of Current Frequency on the Microstructure and Wear Resistance of Ceramic Coatings Embedded with SiC Nano-particles

Produced by Micro-arc Oxidation on AZ91D Magnesium Alloy, J. Mater. Sci. Technol. 26 (2010) 865–871.

[14] M. Daroonparvar, M.A.M. Yajid, N.M. Yusof, H.R. Bakhsheshi-Rad, Preparation and corrosion resistance of a nanocomposite plasma electrolytic oxidation coating on Mg-1%Ca alloy formed in aluminate electrolyte containing titania nano-additives, J. Alloys Compd. 688 (2016) 841–857.

[15] D. Zhang, Y. Gou, Y. Liu, X. Guo, A composite anodizing coating containing superfine Al_2O_3 particles on AZ31 magnesium alloy, Surf. Coat. Technol. 236 (2013) 52–57.

[16] J. Escobar, L. Arurault, V. Turq, Improvement of the tribological behavior of PTFE-anodic film composites prepared on 1050 aluminum substrate, Appl. Surf. Sci. 258 (2012) 8199–8208.

[17] S.V. Gnedenkov, S.L. Sinebryukhov, D.V. Mashtalyar, I.M. Imshinetskiy, Composite fluoropolymer coatings on Mg alloys formed by plasma electrolytic oxidation in combination with electrophoretic deposition, Surf. Coat. Technol. 283 (2015) 347–352.

[18] Z. Wang, L. Wu, Y. Qi, W. Cai, Z. Jiang, Self-lubricating Al2O3/PTFE composite coating formation on surface of aluminium alloy, Surf. Coat. Technol. 204 (2010) 3315–3318.

[19] S. Chen, C. Kang, J. Wang, C. Liu, K. Sun, Synthesis of anodizing composite films containing superfine Al 2 O 3 and PTFE particles on Al alloys, Appl. Surf. Sci. 256 (2010) 6518–6525.

[20] J. Guo, L. Wang, S.C. Wang, J. Liang, Q. Xue, Preparation and performance of a novel multifunctional plasma electrolytic oxidation composite coating formed on magnesium alloy, J. Mater. Sci. 44 (2009) 1998–2006.

[21] X. Lu, C. Blawert, Y. Huang, H. Ovri, M.L. Zheludkevich, Plasma electrolytic oxidation coatings on Mg alloy with addition of SiO_2 particles, Electrochimi. Acta. 187 (2016) 20–33.

[22] X. Lu, C. Blawert, K.U. Kainer, M.L. Zheludkevich, Investigation of the formation mechanisms of plasma electrolytic oxidation coatings on Mg alloy AM50 using particles, Electrochimi. Acta. 196 (2016) 680–691.

[23] X. Lu, C. Blawert, M. Mohedano, N. Scharnagl, M.L. Zheludkevich, K.U. Kainer, Influence of electrical parameters on particle uptake during plasma electrolytic oxidation processing of AM50 Mg alloy, Surf. Coat. Technol. 289 (2016) 179-185.

[24] D. Zhang, G. Dong, Y. Chen, Q. Zeng, Electrophoretic deposition of PTFE particles on porous anodic aluminum oxide film and its tribological properties, Appl. Surf. Sci. 290 (2014) 466–474.

[25] C.L. Beyler, M.M. Hirschler, Thermal Decomposition of Polymers, in: M.J. Hurley, D.T. Gottuk et al. (Eds.), SFPE Handbook of Fire Protection Engineering, Springer-Verlag New York, 2002, pp. 110–131.

[26] F. Wei, W. Zhang, T. Zhang, F. Wang, Effect of variations of Al content on microstructure and corrosion resistance of PEO coatings on MgAl alloys, J. Alloys Compd. 690 (2017) 195–205.
[27] I.C. Cheng, E.G. Fu, L.D. Liu, C.Y. Lee, C.S. Lin, Effect of Fluorine Anions on Anodizing Behavior of AZ91 Magnesium Alloy in Alkaline Solutions, J. Electrochem. Soc. 155 (2008) C219.
[28] Y. Chen, Y. Yang, T. Zhang, W. Zhang, FuhuiWang, X. Lu, et al., Interaction effect between different constituents in silicate-containing electrolyte on PEO coatings on Mg alloy, Surf. Coat. Technol. 307 (2016) 825–836.
[29] K. Tanaka, Y. Uchiyama, S. Toyooka, The mechanism of wear of polytetrafluoroethylene, Wear. 23 (1973) 153–172.
[30] T.A. Blanchet, Y.-L. Peng, S.V. Nablo, Tribology of selectively irradiated PTFE surfaces, Tribol. Lett. 4 (1998) 87–94.

Figure captions

Fig. 1. SEM image of PTFE particles from dried suspension solution.

Fig. 2. Evolution of current of coatings with and without addition of particles during coating formation process.

Fig. 3. SEM images of surface morphology of PEO coatings after 5 min treatment: (a)(c) without PTFE particle, (b)(d) with 20 g/L PTFE particle.

Fig. 4. 3D SEM images and profile of PTFE-containing coatings acquired by Alicon Mex: (a) before wear test; (b) after wear test.

Fig. 5. Surface morphology of coatings treated in PTFE-containing electrolyte for different times: (a) 1min; (b) 2 min; (c) 3min; (d) 5min.

Fig. 6. Backscattered electron (BSE) micrographs of the cross section of the coatings treated in PTFE-containing electrolyte for different times: (a) 1min; (b) 2 min; (c) 3min; (d) 5min.

Fig. 7. X-ray diffraction (XRD) patterns of the particle-containing coatings.

Fig. 8. F, O and P content on the coating surface determined by EDS analysis.

Fig. 9. Friction coefficient of the coatings and Mg substrate during dry sliding wear test.

Fig. 10. EDS mappings of the wear tracks of the coatings: (a) 1min; (b) 2 min; (c) 3min; (d) 5min.

Fig. 11. Schematic diagram of formation of the ridge-like protrusions during PEO process.

Fig. 12. (a) Surface morphology of the coating treated in particle-containing electrolyte with a bubbling generator; (b) Friction coefficient of the coatings.

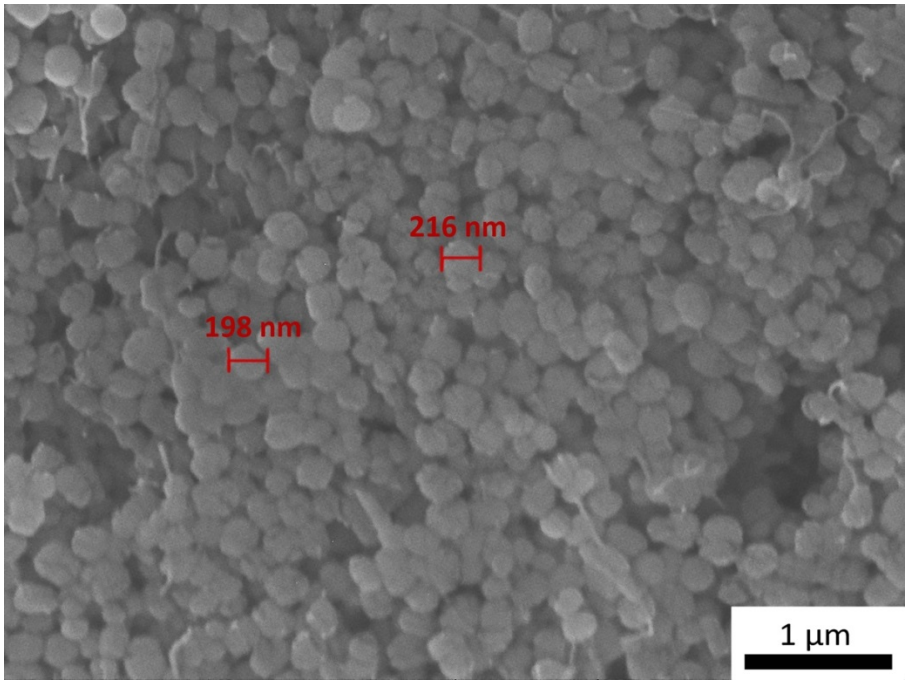

Fig. 1. SEM image of PTFE particles from dried suspension solution.

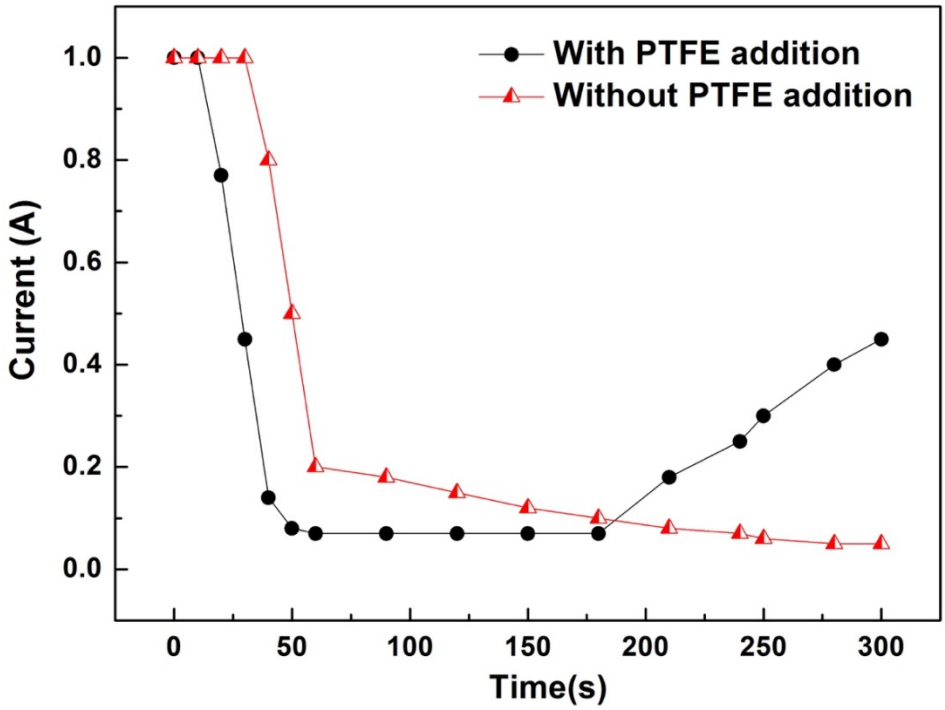

Fig. 2. Evolution of current of coatings with and without addition of particles during coating formation process.

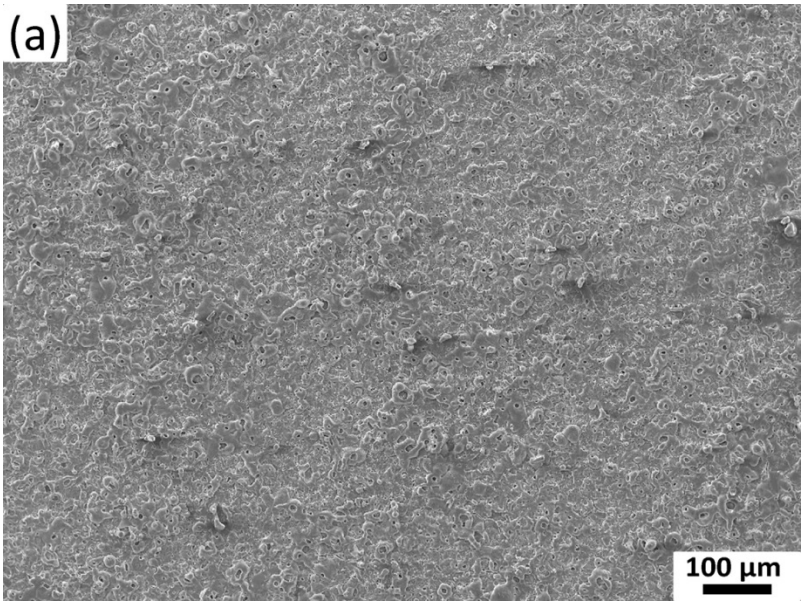
(a)
100 µm

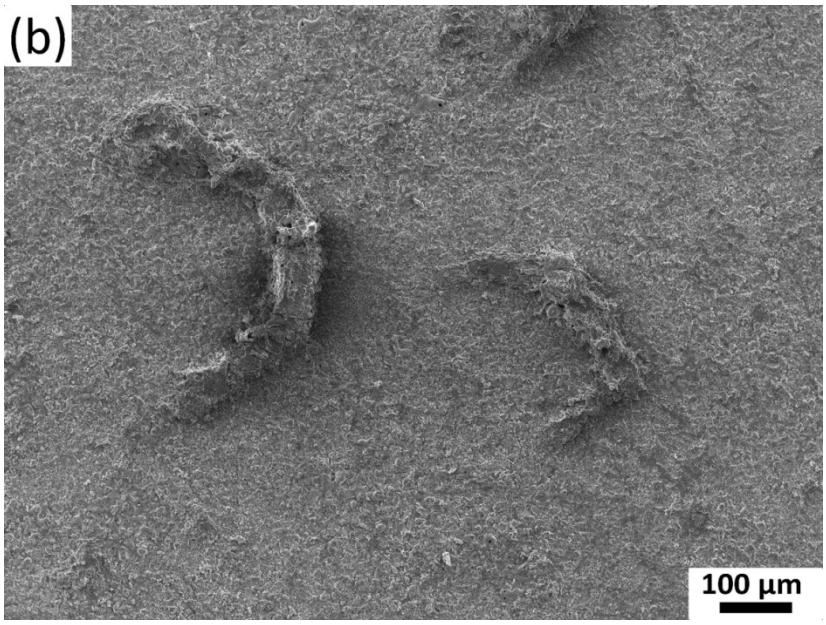
(b)
100 µm

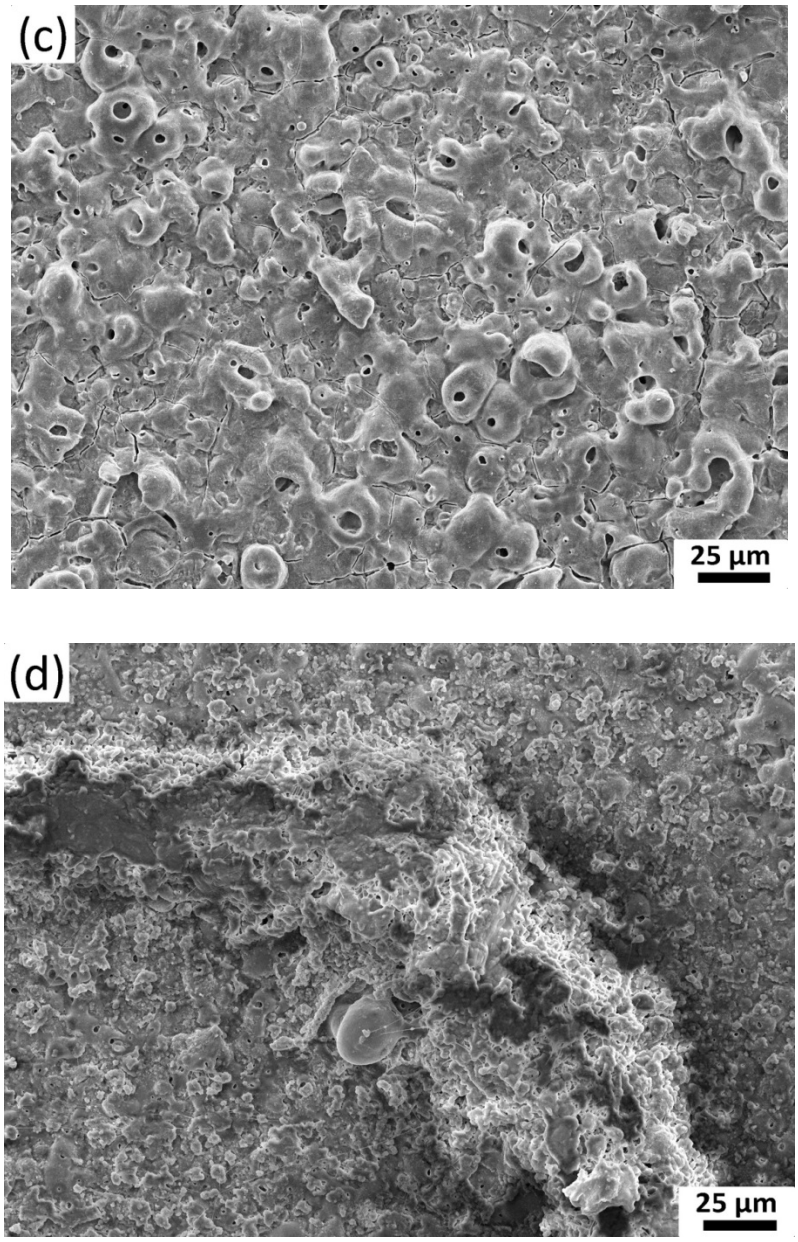

Fig. 3. SEM images of surface morphology of PEO coatings after 5 min treatment: (a)(c) without PTFE particle, (b)(d) with 20 g/L PTFE particle.

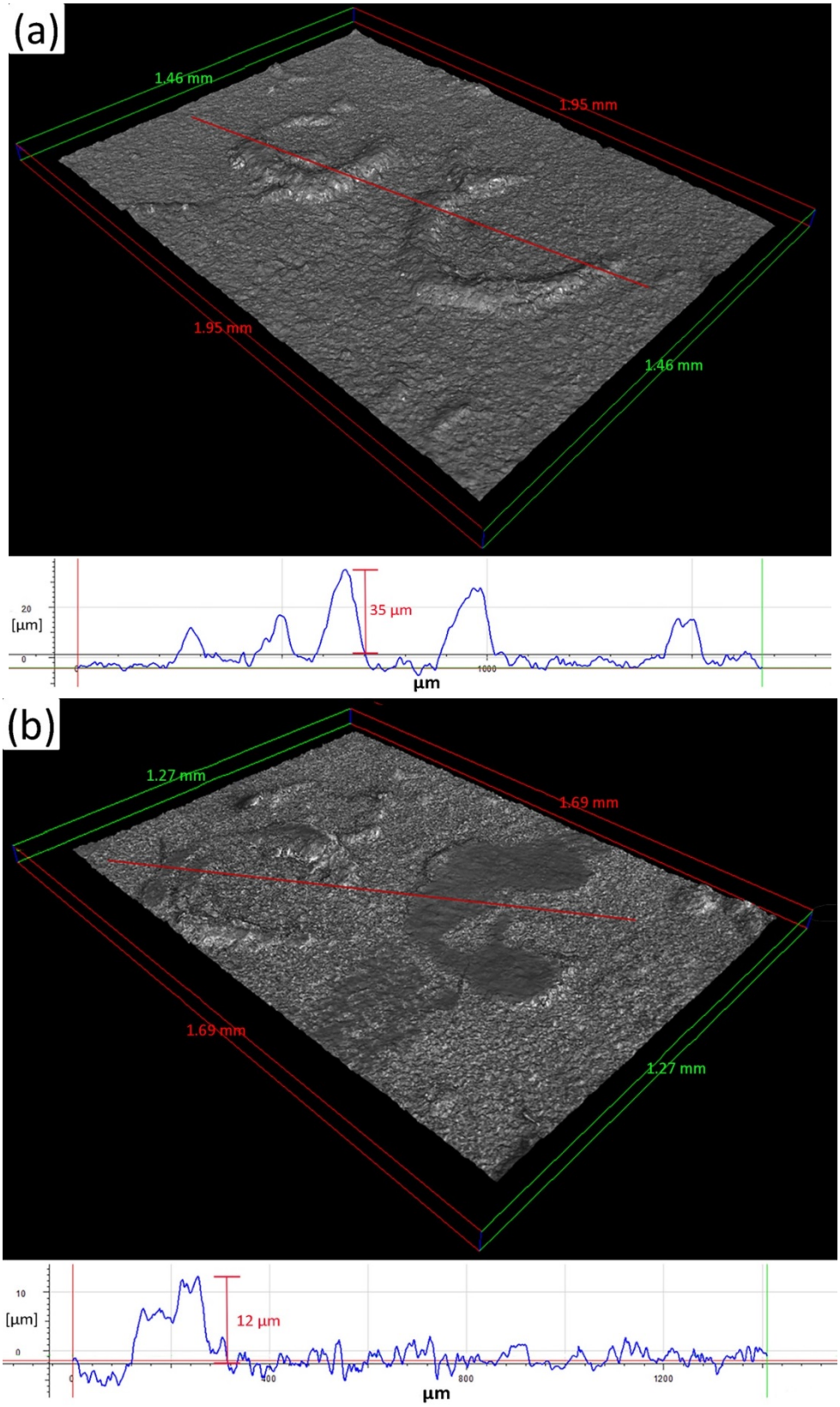

Fig. 4. 3D SEM images and profile of PTFE-containing coatings acquired by Alicon Mex: (a) before wear test; (b) after wear test.

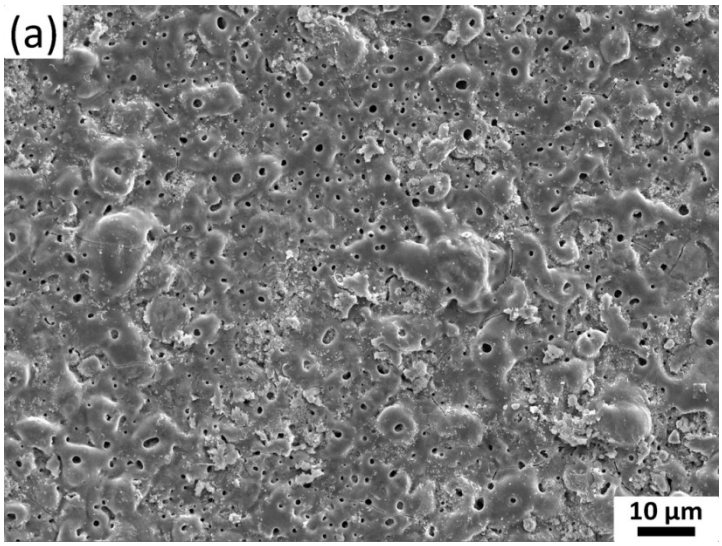
(a)
10 µm

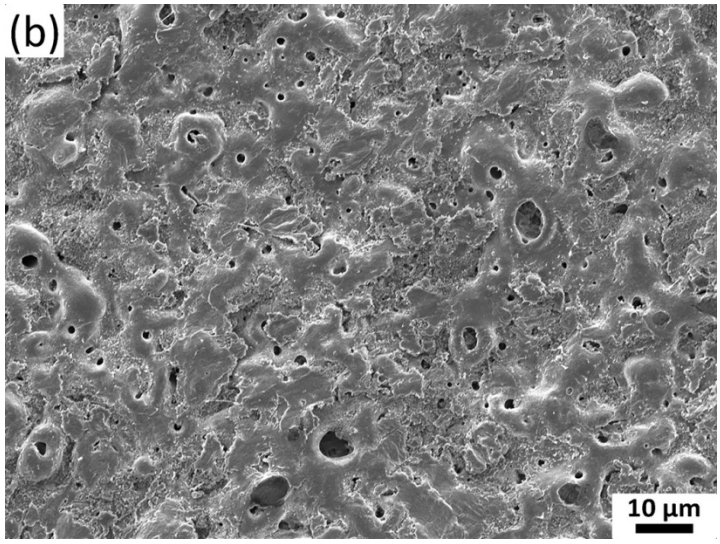
(b)
10 µm

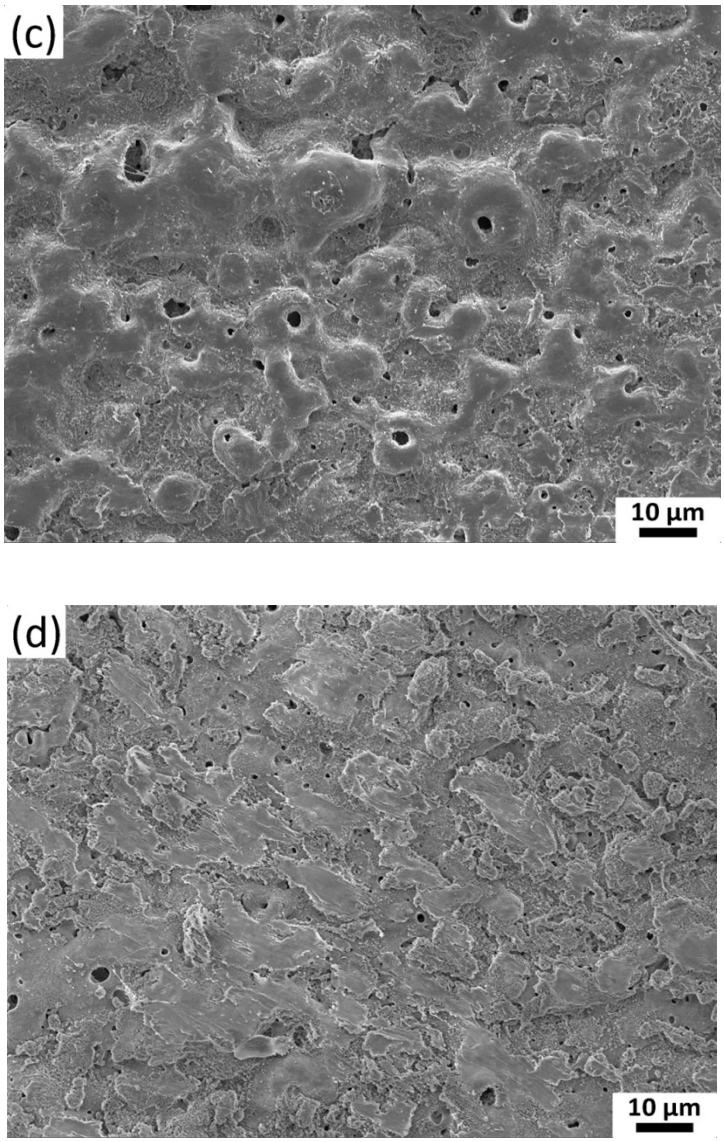

Fig. 5. Surface morphology of coatings treated in PTFE-containing electrolyte for different times: (a) 1min; (b) 2 min; (c) 3min; (d) 5min.

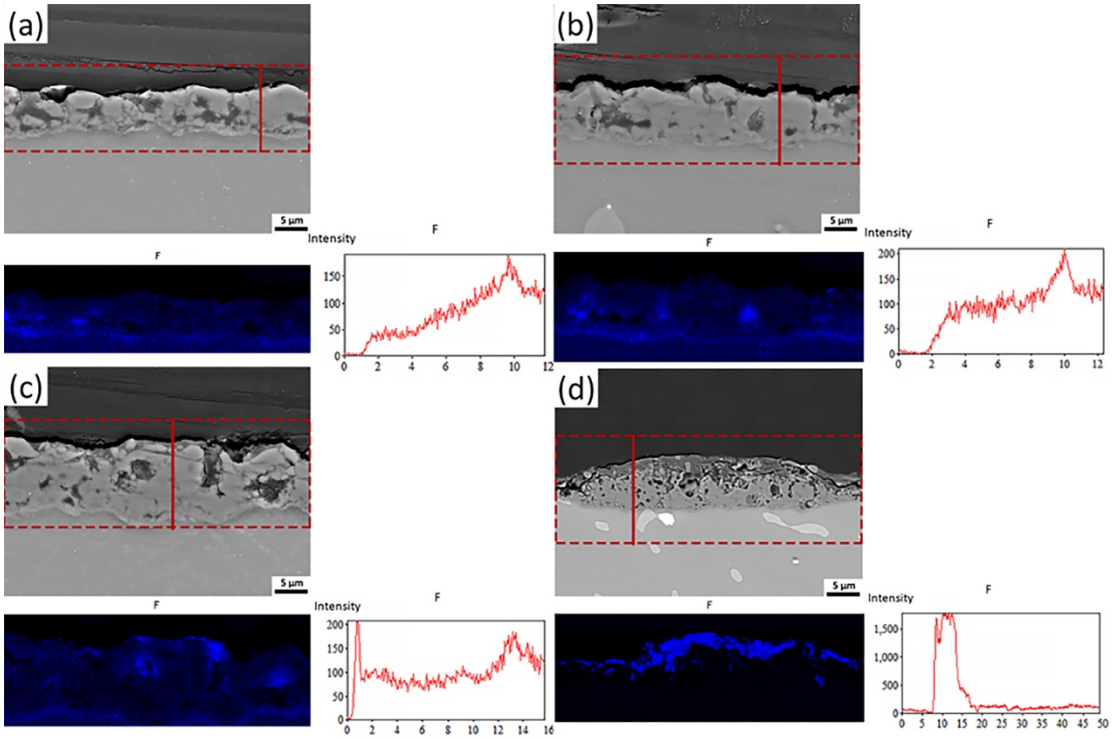

Fig. 6. Backscattered electron (BSE) micrographs of the cross section of the coatings treated in PTFE-containing electrolyte for different times: (a) 1min; (b) 2 min; (c) 3min; (d) 5min.

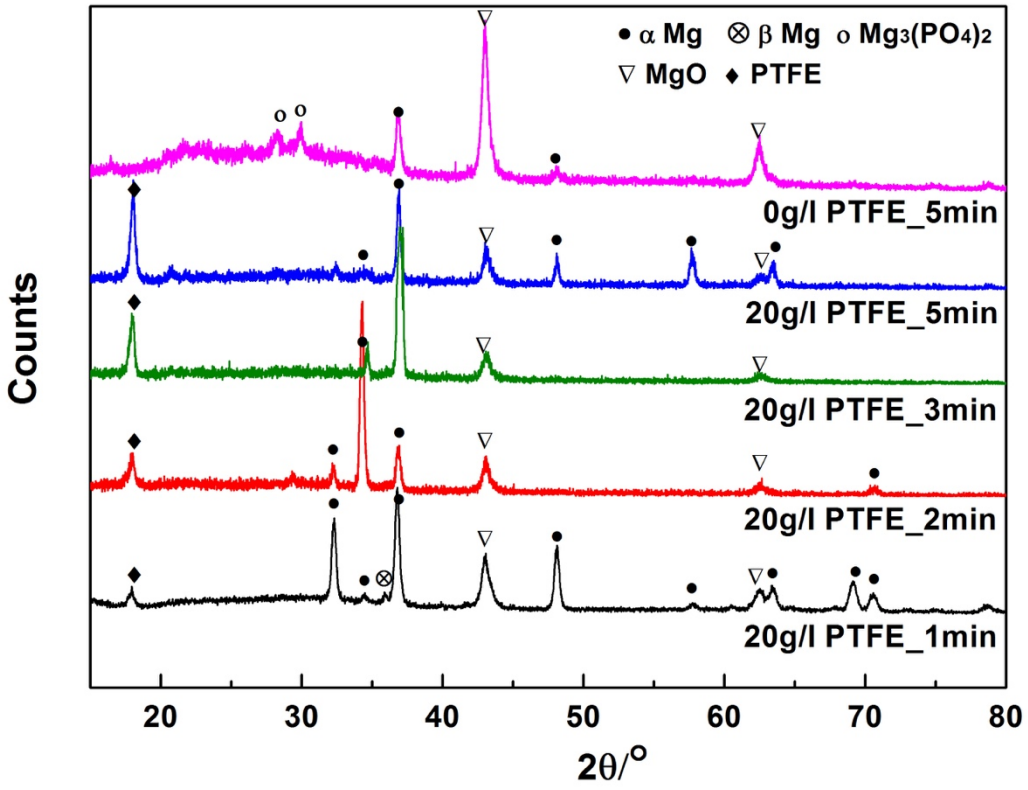

Fig. 7. X-ray diffraction (XRD) patterns of the particle-containing coatings.

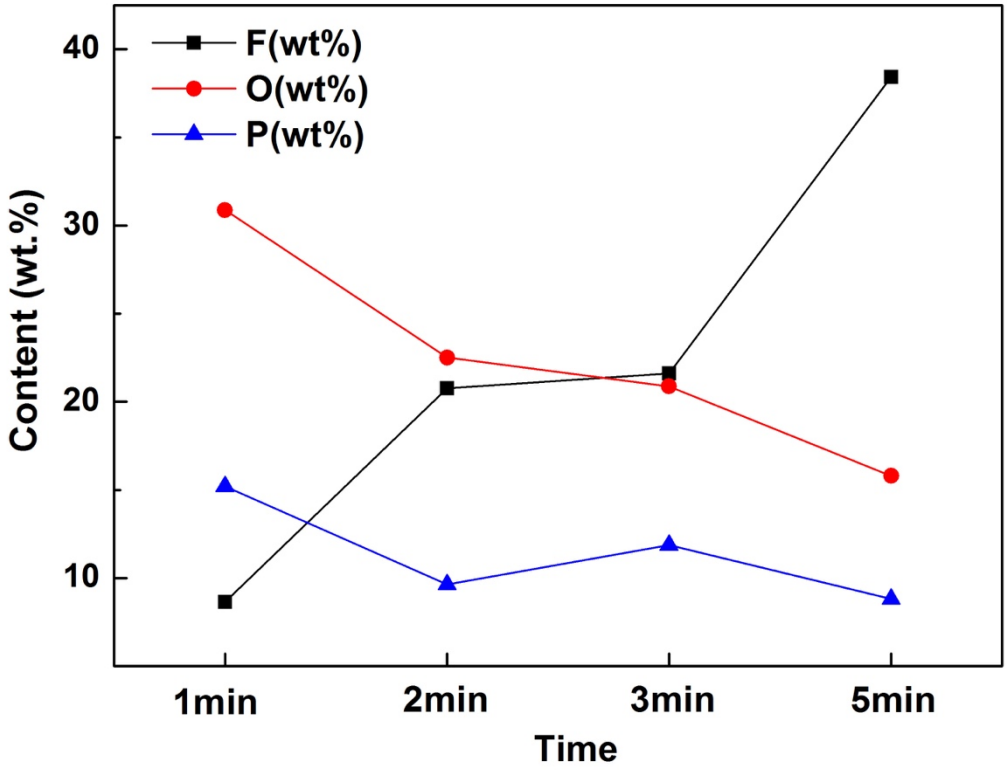

Fig. 8. F, O and P content on the coating surface determined by EDS analysis.

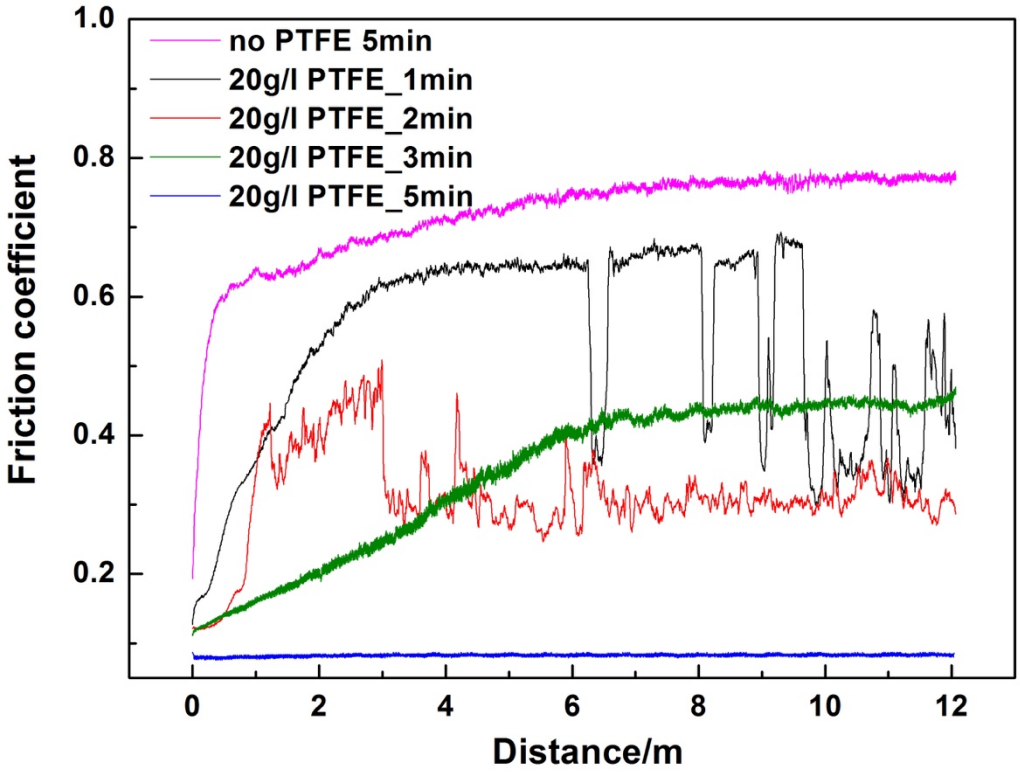

Fig. 9. Friction coefficient of the coatings and Mg substrate during dry sliding wear test.

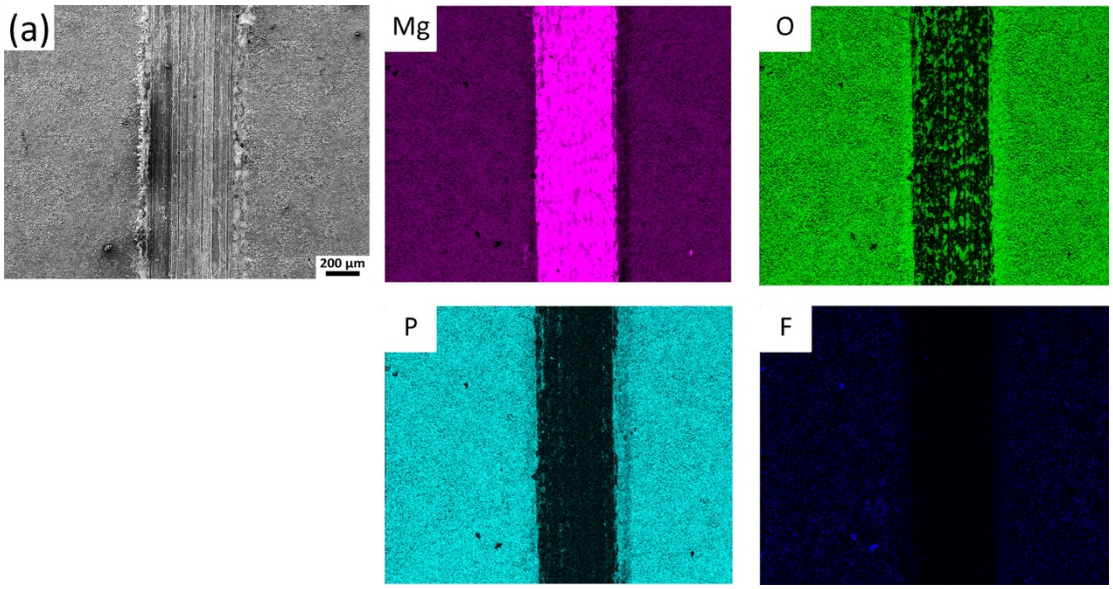
(a)
200 μm
Mg
O
P
F

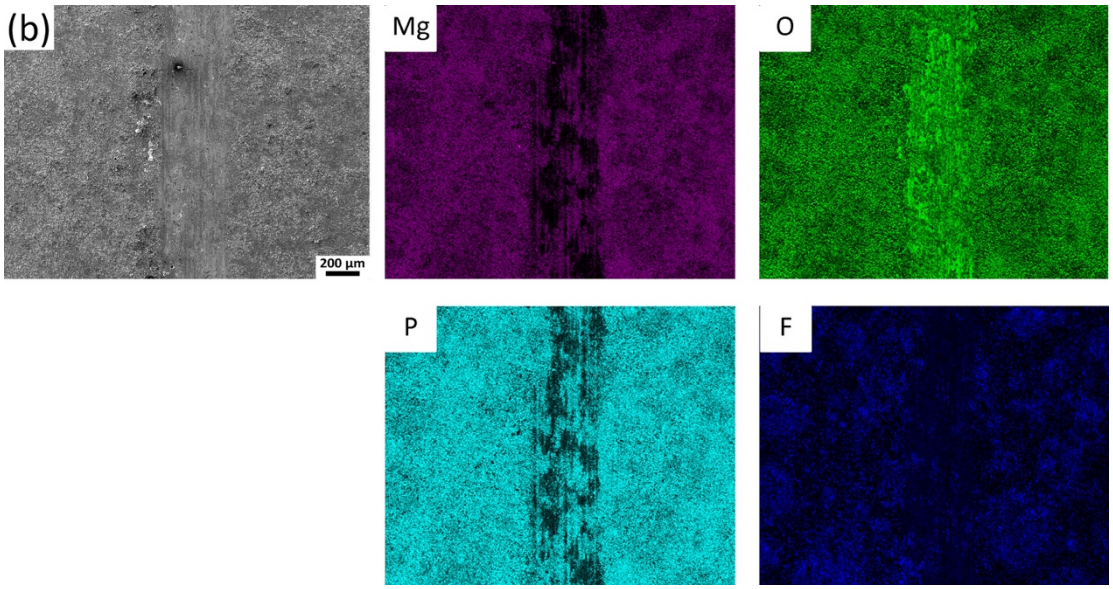
(b)
200 μm
Mg
O
P
F

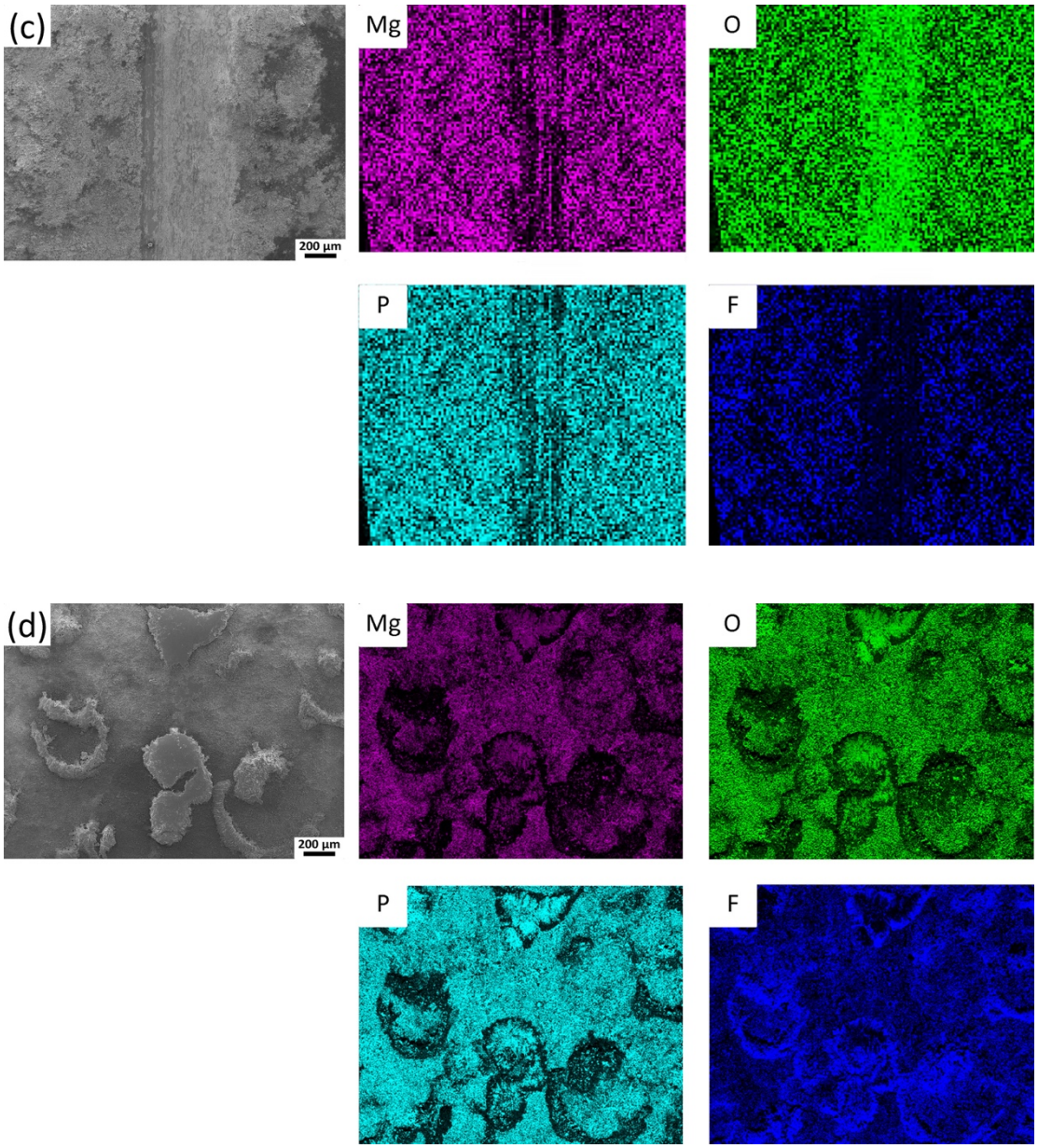

Fig. 10. EDS mappings of the wear tracks of the coatings: (a) 1min; (b) 2 min; (c) 3min; (d) 5min.

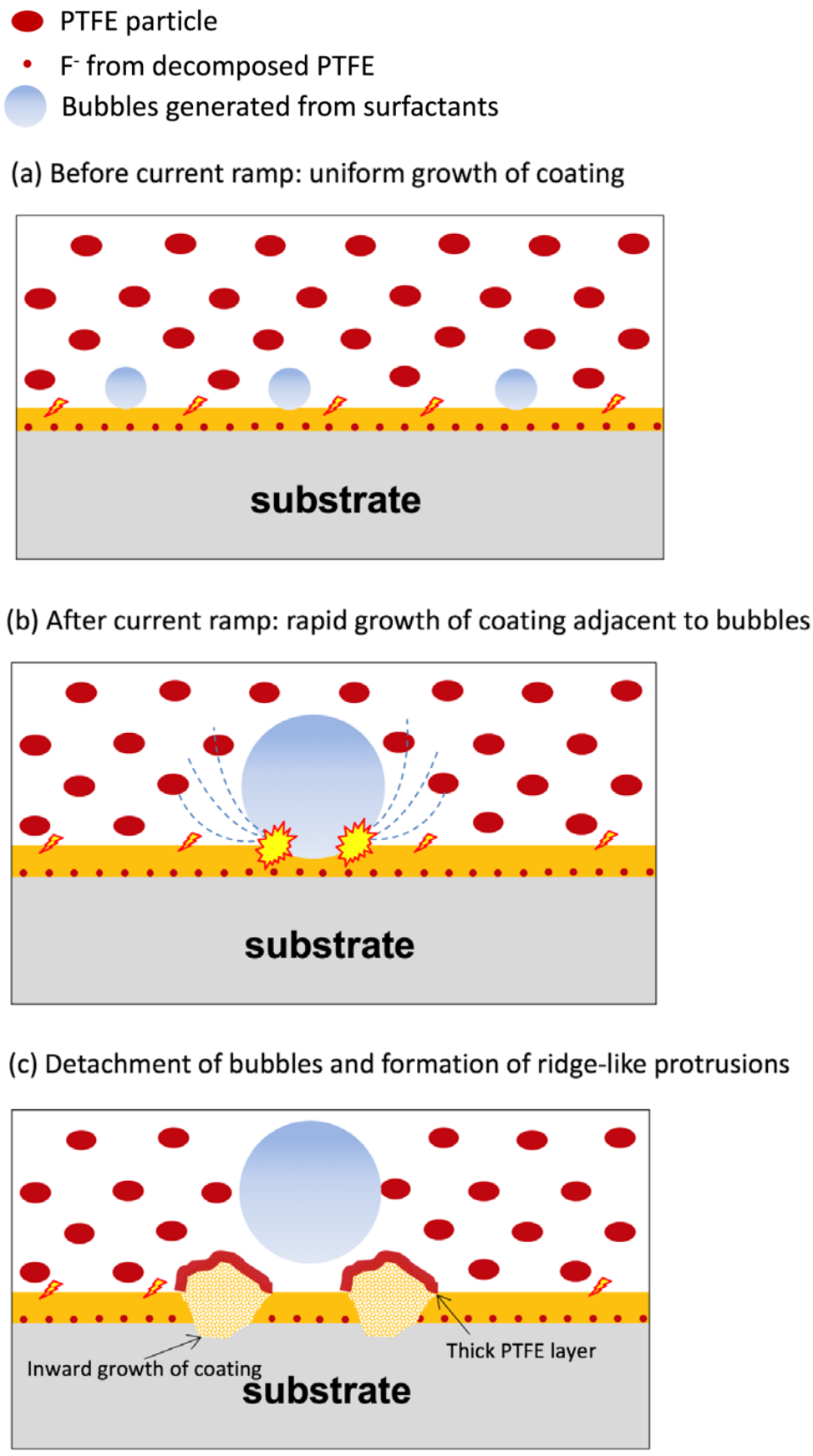

Fig. 11. Schematic diagram of formation of the ridge-like protrusions during PEO process.

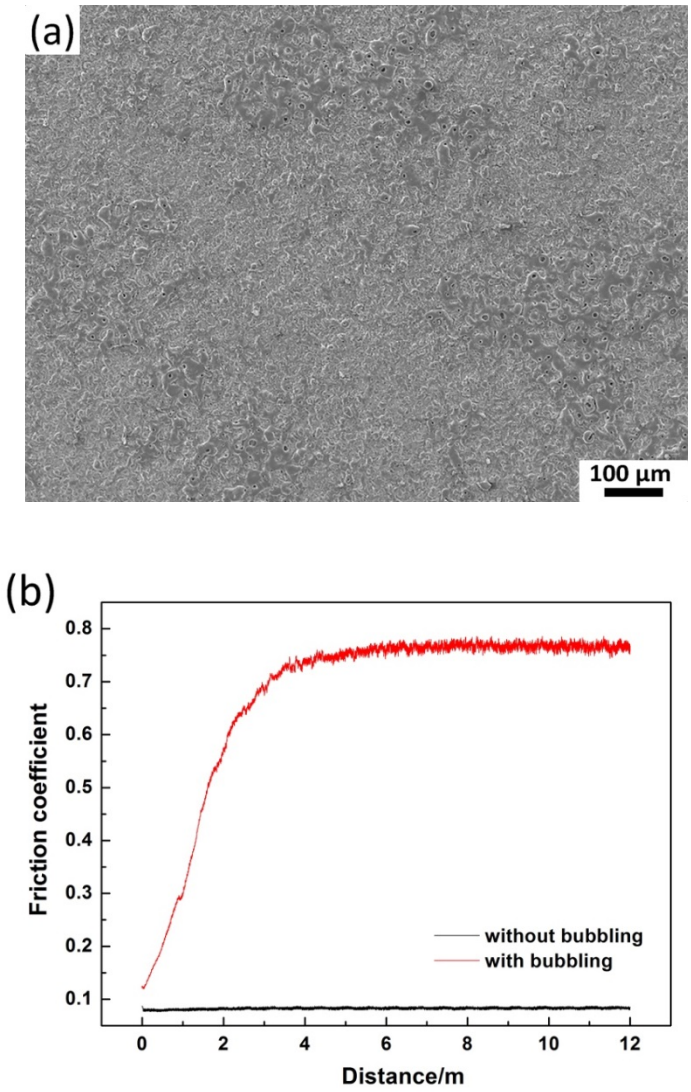

Fig. 12. (a) Surface morphology of the coating treated in particle-containing electrolyte with a bubbling generator; (b) Friction coefficient of the coatings.